Correcting biases in tropical cyclone intensities in low-resolution datasets using dynamical systems metrics

Davide Faranda, Gabriele Messori, Stella Bourdin, Mathieu Vrac, Soulivanh Thao, Jacopo Riboldi, Sebastien Fromang, Pascal Yiou

Correcting biases in tropical cyclone intensities in low-resolution datasets using dynamical systems metrics

Davide Faranda*

Laboratoire des Sciences du Climat et de l'Environnement, CEA Saclay l'Orme des Merisiers, UMR 8212 CEA-CNRS-UVSQ, Université Paris-Saclay & IPSL, 91191, Gif-sur-Yvette, France; London Mathematical Laboratory, 8 Margravine Gardens, London, W6 8RH, UK; LMD/IPSL, Ecole Normale Superieure, PSL research University, 75005, Paris, France

Gabriele Messori

Department of Earth Sciences and Centre of Natural Hazards and Disaster Science (CNDS), Uppsala University, Uppsala, Sweden; Department of Meteorology and Bolin Centre for Climate Research, Stockholm University, Stockholm, Sweden.

Stella Bourdin, Mathieu Vrac, Soulivanh Thao

Laboratoire des Sciences du Climat et de l'Environnement, CEA Saclay l'Orme des Merisiers, UMR 8212 CEA-CNRS-UVSQ, Université Paris-Saclay & IPSL, 91191, Gif-sur-Yvette, France

Jacopo Riboldi

Department of Earth Sciences, Uppsala University, Uppsala, Sweden.

Sebastien Fromang, Pascal Yiou

Laboratoire des Sciences du Climat et de l'Environnement, CEA Saclay l'Orme des Merisiers, UMR 8212 CEA-CNRS-UVSQ, Université Paris-Saclay & IPSL, 91191, Gif-sur-Yvette, France

Corresponding author address: Davide Faranda, Laboratoire des Sciences du Climat et de l'Environnement, CEA Saclay l'Orme des Merisiers, UMR 8212 CEA-CNRS-UVSQ, Université Paris-Saclay & IPSL, 91191, Gif-sur-Yvette, France

E-mail: davide.faranda@lsce.ipsl.fr

ABSTRACT

Although the life-cycle of tropical cyclones is relatively well understood, many of the underlying physical processes occur at scales below those resolved by global climate models (GCMs). Projecting future changes in tropical cyclone characteristics thus remains challenging. We propose a methodology, based on dynamical system metrics, to reconstruct the statistics of cyclone intensities in coarse-resolution datasets, where maximum wind speed and minimum sea-level pressure may not be accurately represented. We base our analysis on 411 tropical cyclones occurring between 2010 and 2020, using both ERA5 reanalysis data and observations from the HURDAT2 database, as well as a control simulation of the IPSL-CM6A-ATM-ICO-HR model. Using ERA5 data, we compute two dynamical system metrics related to the number of degrees of freedom of the atmospheric flow and to the coupling between different atmospheric variables, namely the local dimension and the co-recurrence ratio. We then use HURDAT2 data to develop a univariate quantile–quantile bias correction conditioned on these two metrics, as well as a multivariate correction method. The conditional approach outperforms a conventional univariate correction of the sea-level pressure data only, pointing to the usefulness of the dynamical systems metrics introduced. We then show that the multivariate approach can be used to recover a realistic distribution of cyclone intensities from comparatively coarse-resolution model data.

1. Introduction

Tropical cyclones are among the most devastating natural disasters, often causing fatalities and extensive economic damage (Smith and Katz 2013; Grinsted et al. 2019). They include several collateral hazards that can have significant impacts on people and property, such as rogue waves, flooding, extreme winds, and tornadoes. Combined, these weather events interact to increase the likelihood of loss of life and extensive property damage. The bulk of costs related to tropical cyclones stems from the few, most intense episodes (Emanuel 2021): thus, it is crucial to model such cyclones correctly. Unfortunately, even state-of-the-art global and regional climate models struggle to reproduce the dynamics of the most severe tropical cyclones (Camargo and Wing 2016; Roberts et al. 2020b). This is mainly due to their insufficient resolution, as a grid spacing of the order of few kilometers is needed to model intense cyclones (Rotunno et al. 2009; Moon et al. 2020). Downscaling techniques can be employed to alleviate this issue, but their use is limited by computational costs; furthermore, different downscaling approaches can lead to diverging conclusions (e.g., Caron et al. 2011; Lee et al. 2020; Knutson et al. 2020; Emanuel 2021). The situation is complicated by the reduced length of records in available tropical cyclone data sets, which mostly rely on satellite data not available before the '80s (Chang and Guo 2007): this limitation hinders the emergence from decadal variability of significant changes in tropical cyclone properties (Knutson et al. 2019).

While mid-latitudes synoptic dynamics mostly originate from the chaotic structure of the motions associated with baroclinic instability (Lorenz 1990; Schubert and Lucarini 2015), tropical cyclones are characterized by a rapid organization of convectively unstable flows whose dynamics is turbulent and highly sensitive to boundary conditions (Muller and Romps 2018; Carstens and Wing 2020). Here, we investigate whether it may be possible to exploit this high level of flow

organization to obtain reliable statistics of intense tropical cyclones from relatively coarse-gridded atmospheric data. To achieve this, we compute two metrics that describe cyclones as states of a chaotic high-dimensional dynamical system. The first, d, reflects the dimension (i.e. the number of active degrees of freedom) of an instantaneous state of the cyclone. The second, α, is a proxy for the instantaneous coupling between different atmospheric variables. These metrics have recently provided insights on a number of geophysical phenomena, including transitions between transient metastable states of the mid-latitude atmosphere (Faranda et al. 2017; Hochman et al. 2021), drivers and predictability of extreme events (Hochman et al. 2019; De Luca et al. 2020; Faranda et al. 2020), palaeoclimate attractors (Brunetti et al. 2019; Messori and Faranda 2021) slow earthquake dynamics (Gualandi et al. 2020) and changes in mid-latitude atmospheric predictability under global warming (Faranda et al. 2019). A benefit over previous dynamical systems approaches (e.g Wolf et al. 1985; Cao 1997), is that these metrics can be easily applied to computationally demanding datasets, such as climate reanalyses or climate models.

Applications of d and α in the literature have used a Eulerian approach over a fixed spatio-temporal domain, rather than tracking the evolution of specific physical phenomena. Here, we apply for the first time the two metrics in a semi-Lagrangian perspective to characterize the structure of tropical cyclones in the $d - \alpha$ phase-space. A semi-Lagrangian dynamical systems framework is particularly convenient to study the complex behavior of convectively unstable flow systems (Crisanti et al. 1991; Vulpiani 2010), such as tropical convection. The signature of intense cyclones propagates through scales due to the presence of inverse cascades as suggested by Levich and Tzvetkov (1985) and, more recently, by Faranda et al. (2018); Dunkerton et al. (2009); Tang et al. (2015). Such inverse cascades are associated with potential–kinetic energy conversions and are particularly notable for intense storms (Bhalachandran et al. 2020). Such energy conversions are related to the deep convection in the eyewall, that redistributes to the upper troposphere the

enthalpy gained thanks to surface heat fluxes in the boundary layer: this local process contributes to the generation of the storms' warm core and, ultimately, to wind intensification at the larger, sub-synoptic scale of the storm (Emanuel 1986). We hypothesise that these exchanges have a signature in both the large-scale horizontal velocity and potential vorticity fields, which are reasonably well-represented in coarse simulations or reanalyses. If this indeed holds, it would enable a correction conditioned on d and α of cyclone intensity statistics in datasets where we cannot explicitly access the spatial scales underlying the dynamics of intense tropical cyclones.

We base our analysis on best track cyclone data from the HURDAT2 database, which we take as ground truth, ERA5 reanalysis data and a high-resolution global climate model simulation. We compute the two dynamical systems metrics using the kinetic energy *uv* and the potential vorticity field *PV* at the 850 hPa level. The rationale for using these variables follows the works of Peng et al. (2012) and Fu et al. (2012). The 850 hPa level is chosen because it lies in-between the planetary boundary layer and the middle troposphere, where most of the potential–kinetic energy conversions occur in tropical cyclones (Camargo et al. 2007). The horizontal kinetic energy *uv* is relevant to the study of tropical cyclones because of its direct connection with the wind speed and with the phases of rapid intensification/decay of the cyclones (Krishnamurti et al. 2005). Lower-tropospheric vorticity is frequently used to detect tropical cyclone seeds and relates to their intensification (Davis et al. 2008; Ikehata and Satoh 2021), and PV integrates this knowledge by taking implicitly into account the strength of the warm core, which is related to the vertical stability of the cyclone eye.

Our study is organized as follows: first, we describe the data, variables for cyclone dynamics and the theoretical bases supporting the computation of the dynamical system metrics. Then, we show the general characteristics of the phase space of tropical cyclones in reanalysis data for the different variables, and use these to define a quantile–quantile correction approach for cyclone in-

tensities conditioned on the two dynamical systems metrics. The correction is performed on ERA5 reanalysis, using sea-level pressure (SLP) from HURDAT2 as ground truth. We then conduct an out-of-sample test comparing this approach to an unconditional quantile–quantile correction. Finally, we test this correction on data from a GCM.

2. Data

a. HURDAT2 tropical cyclone data

We follow 197 North Atlantic and 214 Eastern North Pacific tropical cyclones that occurred between 2010 and 2020, using the HURDAT2 Best Track Data (Landsea and Franklin 2013). We use six-hourly information on the location and central pressure of the cyclones, as well as their time of landfall.

b. Representation of tropical cyclones in ERA5 data

We base our analysis on instantaneous[1] $uv = u^2 + v^2$, *SLP* and *PV* at 850hPa from the ERA5 reanalysis (Hersbach et al. 2020), sampled every 6h and additionally whenever the HURDAT2 database displays a cyclone landfall entry – corresponding to a shift in the cyclone dynamics. The horizontal resolution of the data is 0.25°. We also make use of ERA5 data coarse-gridded to a 0.5° horizontal resolution using a nearest neighbour approach. In the vast majority of cases, the SLP difference in the four ERA5 gridpoints around the cyclone core is 1 hPa or less. Using a nearest neighbour approach thus provides similar results to other coarse-graining approaches. The coarse-grained dataset will be hereinafter referred to as ERA5 cg, and will be used to evaluate the sensitivity of our conclusions to the resolution of the dataset. When comparing ERA5 to

[1] We follow here ECMWF's terminology, see: https://confluence.ecmwf.int/pages/viewpage.action?pageId=82870405ERA5:datadocumentation-Table9

HURDAT2, we search for the SLP minimum in ERA5 within a region of 5° of the HURDAT2 cyclone location.

There is often a large discrepancy between the minimum SLP reported in HURDAT2 and that in ERA5 (Fig. 1a,c). Especially for the most intense cyclones, ERA5 systematically underestimates minimum SLP. The biases are larger in the Eastern North Pacific than in the North Atlantic basin (cf. Fig. 1a and 1c). This affects the capability of ERA5 to accurately assign each tropical cyclone to the appropriate Saffir-Simpson category (Simpson and Saffir 1974), which we here use relative to SLP rather than maximum sustained wind (see Table 1. Indeed, recent research argues that SLP is more closely related to cyclone damage than maximum sustained winds (Klotzbach et al. 2020). In particular, ERA5 has a negative bias in the number of tropical cyclones stronger than category 2, namely min(SLP)<980 hPa. While this bias is present in both the North Atlantic and Eastern North Pacific basins, in the latter the biases for the most intense cyclones appear more severe: this might be due to the more intermittent aircraft reconnaissance activity in that basin with respect to the North Atlantic (Knaff et al. 2021). The coarse-graining operation does not notably affect the distribution of cyclone SLP minima (Fig. 1b, d), likely because of the above-mentioned weak SLP variations in the ERA5 dataset in the gridboxes immediately surrounding the cyclone core. We underline that the two ERA5 horizontal resolutions used here are of the same order of magnitude as those of the HighResMIP (High Resolution Model Intercomparison Project, Haarsma et al. 2016) and PRIMAVERA models, which are amongst the current best tools to study climate change impacts on tropical cyclones (Roberts et al. 2020a).

c. Representation of tropical cyclones in IPSL-CM6A-ATM-ICO-HR model data

We use 6-hourly data from the IPSL-CM6A-ATM-ICO model at a horizontal resolution of 0.5°. The simulation we use is a HighResMIP (Haarsma et al. 2016) run lasting for 64 years (1950-

2014). We use the TC tracking algorithm from Ullrich et al. (2021). We additionally remove tracks starting at latitudes above 30°, to minimise incorrect classification of extratropical lows as tropical systems.

The model produces a total of 327 tropical cyclones in the North Atlantic and 989 in the Eastern North Pacific (defined following Knutson et al. 2020). Among them, 150 are randomly sampled for each basin, which is deemed a sufficiently large statistical sample for our analysis. The total number of cyclones reproduced by the IPSL-CM6A-ATM-ICO-HR model is in line with that of other HighResMIP models (cf. Roberts et al. 2020b).

Much like ERA5, the model has a systematic bias in the minimum SLP of the cyclones. A comparison of the distribution of HURDAT2 SLPs with those in the model and in the ERA5 and ERA5 cg data (Fig. 1b, d), suggests that current state-of-the-art GCMs and ERA5 both encounter difficulties when it comes to representing the intensity of tropical cyclones (Kim et al. 2018). Specifically, all three datasets have a sparsely populated left tail of the minimum SLP distribution and, especially for the North Atlantic basin, a different mode when compared to HURDAT2.

3. A dynamical systems view of tropical cyclones

Each instantaneous state of the cyclone, as represented by a given atmospheric variable, corresponds to a point along a phase-space trajectory representing the evolution of the system. We sample this trajectory at discrete intervals determined by the temporal resolution of our data. In our analysis, for every cyclone we adopt 6-hourly domains of size $\sim 1200\,\mathrm{km} \times 1200\,\mathrm{km}$ (41×41 grid points in ERA5 or $\sim 5^\circ$ latitude $\times\ 5^\circ$ longitude), centred at every timestep on the HURDAT2 cyclone location for ERA5 and centered at minimum of sea-level pressure for the simulations. We then consider *PV* and *uv* at 850 hPa in this domain. Our aim is to diagnose the dynamical properties of the instantaneous (in time) and local (in phase-space) states of the cyclone, as represented

by the chosen atmospheric variable and chosen geographical domain (physical space in Fig. 2). To do so, we leverage two metrics issuing from the combination of extreme value theory with Poincaré recurrences (Freitas et al. 2010; Lucarini et al. 2012, 2016).

We consider the sequences of *PV* maps, *uv* maps and pairs maps of the two variables at all timesteps i for all tropical cyclones in our dataset, always centred on their location. The maps are normalised by the respective norms, and we refer to them as PV_i, uv_i and X_i respectively. We thus construct a semi-Lagrangian framework tracking each cyclone. We take each pair of maps X_i in turn as the reference state ζ in our calculation. We then define logarithmic returns as:

$$g(X_i, \zeta) = -\log[\mathrm{dist}(X_i, \zeta)] \tag{1}$$

Here, *dist* is the Euclidean distance between the pairs of maps X_i, but it can be any distance function between two vectors. Since *dist* tends to zero as pairs of X_is increasingly resemble each other, the series of logarithmic returns g_i takes large values for X_i closely resembling ζ.

We next define exceedances as $u(\zeta) = \{t, g(X_i, \zeta) > s(q, \zeta)\}$, where $s(q, \zeta)$ is a high threshold corresponding to the q^{th} quantile of $g(X_i, \zeta)$. These are effectively the previously-mentioned Poincaré recurrences, for the chosen state ζ (phase space in Fig. 2). The Freitas-Freitas-Todd theorem (Freitas et al. 2010; Lucarini et al. 2012) states that the cumulative probability distribution $F(u, \zeta)$ can be approximated by the exponential member of the Generalised Pareto Distribution. We thus have that:

$$F(u, \zeta) \simeq \exp\left[-\frac{u(\zeta)}{\sigma(\zeta)}\right] \tag{2}$$

The parameters u and σ, the scale parameter of the Generalized Pareto Distribution, depend on the chosen state ζ. From the above, we can define the local dimension d as: $d(\zeta) = 1/\sigma(\zeta)$, with $0 < d < +\infty$.

Next, we introduce logarithmic returns and high thresholds separately for PV and uv as $g(PV_i)$, $s_{PV}(q)$ and $g(uv_i)$, $s_{uv}(q)$ respectively. These allow us to define the co-recurrence ratio (α) as:

$$\alpha(\zeta) = \frac{\nu[g(PV_i) > s_{PV}(q) \mid g(uv_i) > s_{uv}(q)]}{\nu[g(X_i) > s_{PV}(q)]} \tag{3}$$

with $0 \leq \alpha \leq 1$. Here, $\nu[-]$ is the number of events satisfying condition $[-]$, and all other variables are defined as before. By definition, α is symmetric with respect to the choice of variable (PV or uv), since $\nu[g(PV_i) > s_{PV}(q)] \equiv \nu[g(uv_i) > s_{uv}(q)]$.

While the derivation of d and α may seem very abstract, the two metrics can be related intuitively to the physical properties of the tropical cyclones. d is a proxy for the active number of degrees of freedom of the cyclones' instantaneous states, while α measures the coupling between different variables. The relationship between dynamical systems metrics and the structure of tropical cyclones is elucidated in Figure 3. d and α are anti-correlated: low dimensionality is generally associated to a high coupling between the PV and uv maps, while the opposite holds for high dimensionality (Fig. 3a). Most of the considered time steps fall in a regime of relatively low dimensionality relative to the number of gridpoints in the lagrangian domain (41^2), and of low coupling. We first investigate the uv and PV atmospheric patterns corresponding to these timesteps. To do so, we consider all points below the 0.95 quantiles of the d and α distributions, corresponding to thresholds of d_H=30 and α_H=0.35. These data show a clear, albeit relatively weak, cyclonic structure in PV, with values peaking at $\sim$2 PVU (Fig. 3b). The uv pattern also reflects a cyclonic structure, with values peaking at $\sim$ 12 m s^{-1} (Fig. 3e). The picture is radically different for cyclone timesteps with $d > d_H$ or $\alpha > \alpha_H$ (Fig. 3c,d,f,g). High values of d feature

a smaller, weaker PV core than the bulk of the data, which is reflected in low values of kinetic energy (Fig. 3c,f). High values of α instead correspond to an intense cyclonic PV core and a correspondingly intense KE structure around it (Figs. 3d,g). The same qualitative features emerge also for the ERA5 cg and HighResMIP data (not shown).

These results reflect the strong coupling between dynamic and thermodynamic fields in intense cyclones (e.g., Emanuel 1986, 1997; Montgomery and Smith 2017) – the thermodynamics partly encapsulated by the PV structure of the cyclones' core. Intense tropical cyclones display a quasi-axisymmetric shape, a state where very few degrees of freedom (i.e., low d values, which typically correspond to high α values) are needed to describe their dynamics because of the air parcels all aligning with the cyclones' global rotation. On the contrary, the cyclones with higher dimensionality likely display asymmetric or multiple PV patches, with a less organised KE landscape.

The connection between d, α and cyclone intensity holds in general when diagnosing the intensity of the cyclones using the minimum SLP, computed from gridded data (Fig. 4). In general, large values of α (colorscale) correspond to low values of the minimum SLP in both the North Atlantic and Eastern North Pacific basins. Moreover, the most intense tropical cyclones phases are marked by a low dimension d. Similar conclusions hold for the HighResMIP data, as further discussed in Sect. 4b. Remarkably, the coarse-graining operation on ERA5 data does not alter sensibly the dynamical properties d and α and they maintain roughly the same range of values of the original 0.25° reanalysis (Fig. 4b, d). The explanation for this stability follows that given in Faranda et al. (2017) for the SLP data over the North-Atlantic: the dynamical systems metrics are practically insensible to resolution, provided that the resolution is sufficient to

represent the underlying dynamics of the data. This is the case here since, as previously discussed, ERA5 cg and ERA5 share near-identical distributions of cyclone SLP minima.

4. Bias Corrections of tropical cyclone sea-level pressure minima

a. Bias Corrections of ERA5 tropical cyclone sea-level pressure minima

We perform two bias corrections for ERA5 minimum sea-level pressure. In both cases we prepare our data as follows. Firstly, we rearrange our set of tropical cyclones by alphabetic order. This mixes tropical cyclones from different years and different parts of the cyclone season in the training and in the verification datasets. We thus avoid intraseasonal effects and possible non-stationarities linked to anthropogenic climate change or interannual variability of the atmospheric circulation. Then we consider the first 4000 datapoints of our rearranged HURDAT2 SLP minima for each basin as training data and the remaining 2029 datapoints for the North Atlantic basin and 2313 datapoints for the Eastern North Pacific basin as verification data. This same split is also applied to ERA5 cg.

We next define objective metrics to determine whether our bias corrections improve the cyclone intensities. We use the original Simpson and Saffir (1974) scale of tropical cyclones category based on the SLP minima and compute them for the verification datasets (Table 1). We define two error metrics: the total count of tropical cyclones time-steps with wrong category Err_T, and the count of major tropical cyclones (intensity$\geq$3) with wrong category Err_C.

The first bias correction we implement is an unconditional quantile-quantile correction. We begin by subtracting the median of the distributions of SLP minima from the data, which we then add back at the end of the procedure. We then compute the difference $\Delta(q)$ between the empirical cumulative density functions (ECDFs) of SLP minima in HURDAT2 with respect to ERA5 and ERA5 cg evaluated at 100 quantile values q. For each data to correct, the closest quantile $q*$ in the ECDF(ERA5) or ECDF(ERA5 cg) dataset is found and the value $\Delta(q*)$ is added to the original value.

The second bias correction approach is conditioned on the dynamical systems metrics. The results presented in Figures 3 and 4 show that we can discriminate intense tropical cyclones as those having a large value of α and a small value of d. We test several d_H–α_H value pair (using the same convention of Fig.3) to separate the training dataset into intense ($d < d_H$, $\alpha > \alpha_H$) and non-intense cyclones. We then apply the previously described quantile-quantile correction to the two subsets of cyclones separately. We then use a grid-search approach to select the d_c–α_c value pair minimizing the total error. We scan all combinations of $10 \leq d \leq 38$ and $0.1 \leq \alpha \leq 0.34$, with resolution $\Delta d = 1$ and $\Delta\alpha = 0.1$. Results are displayed in Figures 5-6 for the ERA5 and ERA5 cg datasets respectively. The upper (resp. lower) horizontal planes show the error metrics for the non corrected (resp. corrected without dynamical systems metrics) data. The curved surfaces show the the errors when bias correction is performed using the dynamical systems metrics. Panels (a,b) show Err_T for the North Atlantic and Eastern North Pacific basins respectively, while panels (c,d) show the metric Err_C. In all cases and for both the ERA5 and ERA5 cg datasets the conditional bias correction greatly improves the identification of the tropical cyclones category relative to the uncorrected data. Furthermore, there are large areas of the d–α plane where the conditional bias correction improves the results of the unconditional correction. We select the values d_c and

α_c that minimise the total error $Err = Err_T(ATL) + Err_T(ENP) + Err_C(ATL) + Err_C(ENP)$. We additionally impose that the chosen values improve upon the unconditional correction for both basins and both Err_T and Err_C. This analysis yield $d_c = 15$ and $\alpha_c = 0.11$ for ERA5 and $d_c = 18$,$\alpha_c = 0.13$ for ERA5 cg. As already noted in Fig. 1a,c, the biases for the most intense cyclones are more severe in the Eastern North Pacific. While the bias correction improves the situation, both Err_C and Err_T for the Eastern North Pacific remain larger than for the North Atlantic.

We illustrate in detail the improvement obtained with the two bias correction approaches in Figures 7-8. Panels (a,e) show that the ECDFs of bias- corrected SLPs are closer to the verification dataset HURDAT2 than the non-corrected ones. Similarly, panels (b,f) show that the correspondence of observed versus modelled SLPs for individual cyclones is improved by the bias correction. However, for many of the tropical cyclone timesteps, the bias correction attributes a higher category than the original data. This is shown in panels (c,g) in terms of Δ between the categories as estimated for ERA5 (cg) data relative to HURDAT2. Finally panels (d,h) show the evident improvements in terms of intensity histograms: the original non corrected data do not have any category 4 or 5 tropical cyclones, whereas with the corrections we are able to retrieve the full intensity spectrum. The difference between ERA5 and ERA5 cg is limited, although panels (d,h) evidence that the coarse-graining does have some effect on the most intense cyclones. As previously noted, a clear difference emerges between the North Atlantic and Eastern North Pacific basins, with the latter showing larger biases for both the uncorrected and corrected data.

b. Bias Corrections of HighResMip tropical cyclone sea-level pressure minima

When looking at the cyclone SLP minima for the HighResMIP data, we remark immediately the virtual lack of minima below 960 hPa and the reduced range of d and α values compared to ERA5 or ERA5 cg data (cf. Fig. 9a,c, and 4). These results point to a different dynamical representation of tropical cyclones in HighResMIP. The consequence is that the statistical dependencies between SLP, d and α in HighResMIP are not the same as in the reference data (ERA5 and HURDAT). Up to now, the unconditional and conditional bias correction methods applied to adjust cyclone properties were univariate. Hence, dependencies between the three variables (i.e. SLP minima, d and α) were not corrected by the unconditional approach, and only partly with the conditional one. Thus, the resulting tri-variate dependence structures were likely not appropriately represented by the corrected data. To account for this, we now also make use of a multivariate bias correction (MBC) method to adjust not only the univariate distributions but also the dependence between the three variables of interest. To do so, the "Rank Resampling for Distributions and Dependencies" (R2D2) method is applied to adjust jointly (SLP minima, d, alpha). R2D2 relies on an analogue-based method applied to the ranks of the time series to be corrected rather than to their "raw" values (Vrac 2018). This MBC method can be easily designed to adjust both inter-variable, inter-site and temporal properties (Vrac and Thao 2020) but is used only in its inter-variable configuration in the present study. Figure 9 shows the scatterplots of minimum SLP vs local dimension d and co-recurrence ratio α without (a,c) and with (b,d) R2D2 correction. The R2D2 correction enables to retrieve SLP minima of order 920 hPa as well as extend the range of values of d and α, reproducing a pattern closer to the one observed in ERA5.

We next apply the unconditional and conditional bias-correction methodologies, as well as the R2D2 method to the HighResMIP simulations. The main difference here is that the correction has

to be fitted and applied directly to free-running HighResMIP simulations. In such a context, cross-validation techniques for corrections evaluation have been recently heavily criticized (Maraun and Widmann 2018) due to the influence of the model internal variability on the correction results. Hence, in the following, no separation into training and test data is performed: we correct the bulk cyclone statistics for all selected cyclones in the IPSL-CM6A-ATM-ICO-HR year-long simulation. We first estimate the ECDFs and compute the Δ function between HighResMIP and HURDAT2 data. We then correct the full dataset using the unconditional, conditional on α, d – using the ERA5 cg values d_c and α_c – and R2D2 corrections. The results are shown in Figure 10. For the ECDFs (panels a,c), corrections obtained using or not the dynamical systems metrics seem comparable and improve, once again, the distribution of SLP minima. When looking at the tropical cyclone intensities (panels b,d) we observe that the R2D2 correction of SLP minima allows to recover a distribution of intensities which is very close to that of the HURDAT2 data. This suggests that, when applying R2D2, we are able to take into full account the information provided by the two dynamical systems metrics.

5. Implications of the results for the numerical simulation of tropical cyclones

Starting from the observation that gridded datasets of tropical cyclones have a large bias in the representation of the intensity of extreme cyclones, we have introduced a procedure to bias correct them. We have used: i) an unconditional quantile–quantile correction of the sea-level pressure minima of cyclones timesteps towards the HURDAT2 reference dataset; ii) a correction conditioned on two dynamical systems metrics (dimension and co-recurrence ratio); and iii) the R2D2 correction. When using the dynamical systems metrics, we use the dynamical information from an underlying reduced phase space incorporating horizontal kinetic energy *uv* and potential vorticity *PV* at 850 hPa. We have observed that the dynamical systems metrics are able to track

intense cyclones as organized states of the dynamics, yielding low dimensions and high dynamical/thermodynamic coupling. While all bias corrections improve the bulk statistics of tropical cyclone intensity representation in the ERA5 reanalysis and in the IPSL-CM6A-ATM-ICO-HR HighResMIP model, the categorisation for individual cyclones is not always improved. For the ERA5 reanalyses, we find that the conditional bias-correction improves over its unconditional counterpart. For the HighResMIP model, the best bias correction is the multivariate R2D2 correction which takes into account the relationships among SLP, d and α. This suggests that accounting for the multivariate dependence structures associated to the dynamical systems metrics is crucial to correcting the distribution of tropical cyclone intensities.

These considerations have a number of concrete implications for current research on tropical cyclones. Current GCMs — and even reanalysis products — struggle in reproducing minimum sea-level pressures comparable to those observed. Our study offers a way of mapping intense cyclones in d, α space and a procedure to correct biases in century-long reanalysis products to perform climate change studies of their intensity. This, in turn, may provide a strategy for studying changes in tropical cyclone intensity driven by anthropogenic forcing. Indeed, while d and α may not be used to provide a deterministic indication of cyclone intensity, they do provide a robust constraint for statistical correction, especially in reanalysis data. The large range of local dimensions associated with the dynamics of different phases of tropical cyclones may explain why it is so difficult to adequately represent them in numerical models. Follow-up studies will include the use of a larger set of HighResMIP data under different forcing scenarios, to test systematically whether the dynamical systems bias correction may be successfully applied to model data. The bias correction procedures will then be adapted to take into account the non-stationarities introduced by anthropogenic forcing, e.g. by replacing the quantile-quantile mapping with a CDF-t

correction (Vrac et al. 2012) allowing to account for climate change in the correction procedure. A further avenue for future work will be to move from the pointwise correction of minimum SLP performed here, to correcting the spatial structure of the field, using multivariate bias correction techniques (e.g. Cannon 2018; Vrac 2018; Robin et al. 2019; Vrac and Thao 2020) or tools from machine learning (e.g. François et al. 2021).

Acknowledgments. The authors acknowledge the support of the INSU-CNRS-LEFE-MANU grant (project DINCLIC), as well as the grant ANR-19-ERC7-0003 (BOREAS). This work has received support from the European Union's Horizon 2020 research and innovation programme (Grant agreement No. 101003469, XAIDA) and from the European Research Council (ERC) under the European Union's Horizon 2020 research and innovation programme (Grant agreement No. 948309, CENÆ project). MV was partly supported by the "COESION" project funded by the French National program LEFE (Les Enveloppes Fluides et l'Environnement), as well as the French National "Explore2" project funded by the French Ministry of Ecological Transition (MTE) and the French Office for Biodiversity (OFB).

References

Bhalachandran, S., D. R. Chavas, F. D. M. Jr, S. Dubey, A. Shreevastava, and T. N. Krishnamurti, 2020: Characterizing the Energetics of Vortex-Scale and Sub-Vortex-Scale Asymmetries during Tropical Cyclone Rapid Intensity Changes. *Journal of the Atmospheric Sciences*, **77 (1)**, 315–336, doi:10.1175/JAS-D-19-0067.1, URL https://journals.ametsoc.org/view/journals/atsc/77/1/jas-d-19-0067.1.xml, publisher: American Meteorological Society Section: Journal of the Atmospheric Sciences.

Brunetti, M., J. Kasparian, and C. Vérard, 2019: Co-existing climate attractors in a coupled aqua-planet. *Climate Dynamics*, **53 (9-10)**, 6293–6308.

Camargo, S. J., K. A. Emanuel, and A. H. Sobel, 2007: Use of a genesis potential index to diagnose ENSO effects on tropical cyclone genesis. *Journal of Climate*, **20 (19)**, 4819–4834.

Camargo, S. J., and A. A. Wing, 2016: Tropical cyclones in climate models. *WIREs Clim. Change*, **7**, 211–237, doi:https://doi.org/10.1002/wcc.373.

Cannon, A. J., 2018: Multivariate quantile mapping bias correction: an n-dimensional probability density function transform for climate model simulations of multiple variables. *Climate dynamics*, **50 (1)**, 31–49.

Cao, L., 1997: Practical method for determining the minimum embedding dimension of a scalar time series. *Physica D: Nonlinear Phenomena*, **110 (1-2)**, 43–50.

Caron, L. P., C. Jones, and K. Winger, 2011: Impact of resolution and downscaling technique in simulating recent Atlantic tropical cylone activity. *Clim. Dyn.*, **37**, 869–892, doi:doi.org/10.1007/s00382-010-0846-7.

Carstens, J. D., and A. A. Wing, 2020: Tropical cyclogenesis from self-aggregated convection in numerical simulations of rotating radiative-convective equilibrium. *Journal of Advances in Modeling Earth Systems*, **12 (5)**, e2019MS002 020.

Chang, E. K., and Y. Guo, 2007: Is the number of north atlantic tropical cyclones significantly underestimated prior to the availability of satellite observations? *Geophysical Research Letters*, **34 (14)**.

Crisanti, A., M. Falcioni, A. Vulpiani, and G. Paladin, 1991: Lagrangian chaos: transport, mixing and diffusion in fluids. *La Rivista del Nuovo Cimento (1978-1999)*, **14 (12)**, 1–80.

Davis, C., C. Snyder, and A. C. Didlake Jr, 2008: A vortex-based perspective of eastern pacific tropical cyclone formation. *Monthly weather review*, **136 (7)**, 2461–2477.

De Luca, P., G. Messori, F. M. Pons, and D. Faranda, 2020: Dynamical systems theory sheds new light on compound climate extremes in europe and eastern north america. *Quarterly Journal of the Royal Meteorological Society*, **146 (729)**, 1636–1650.

Dunkerton, T. J., M. Montgomery, and Z. Wang, 2009: Tropical cyclogenesis in a tropical wave critical layer: Easterly waves. *Atmospheric Chemistry and Physics*, **9 (15)**, 5587–5646.

Emanuel, K., 2021: Response of global tropical cyclone activity to increasing CO2: Results from downscaling CMIP6 models. *J. Climate*, **34**, 57–70, doi:10.1175/JCLI-D-20-0367.1.

Emanuel, K. A., 1986: An air-sea interaction theory for tropical cyclones. part i: Steady-state maintenance. *Journal of Atmospheric Sciences*, **43 (6)**, 585–605.

Emanuel, K. A., 1997: Some aspects of hurricane inner-core dynamics and energetics. *Journal of the Atmospheric Sciences*, **54**, 1014–1026, doi:10.1175/1520-0469(1997)054⟨1014:SAOHIC⟩2.0.CO;2.

Faranda, D., M. C. Alvarez-Castro, G. Messori, D. Rodrigues, and P. Yiou, 2019: The hammam effect or how a warm ocean enhances large scale atmospheric predictability. *Nature communications*, **10 (1)**, 1–7.

Faranda, D., V. Lembo, M. Iyer, D. Kuzzay, S. Chibbaro, F. Daviaud, and B. Dubrulle, 2018: Computation and characterization of local subfilter-scale energy transfers in atmospheric flows. *Journal of the Atmospheric Sciences*, **75 (7)**, 2175–2186.

Faranda, D., G. Messori, and P. Yiou, 2017: Dynamical proxies of north atlantic predictability and extremes. *Scientific reports*, **7**, 41 278.

Faranda, D., G. Messori, and P. Yiou, 2020: Diagnosing concurrent drivers of weather extremes: application to warm and cold days in north america. *Climate Dynamics*, **54 (3)**, 2187–2201.

François, B., S. Thao, and M. Vrac, 2021: Adjusting spatial dependence of climate model outputs with cycle-consistent adversarial networks. *Climate Dynamics*, **57 (11)**, 3323–3353.

Freitas, A. C. M., J. M. Freitas, and M. Todd, 2010: Hitting time statistics and extreme value theory. *Probability Theory and Related Fields*, **147 (3-4)**, 675–710.

Fu, B., M. S. Peng, T. Li, and D. E. Stevens, 2012: Developing versus nondeveloping disturbances for tropical cyclone formation. part ii: Western north pacific. *Monthly weather review*, **140 (4)**, 1067–1080.

Grinsted, A., P. Ditlevsen, and J. H. Christensen, 2019: Normalized US hurricane damage estimates using area of total destruction, 1900- 2018. *Proceedings of the National Academy of Sciences*, **116 (48)**, 23 942–23 946.

Gualandi, A., J.-P. Avouac, S. Michel, and D. Faranda, 2020: The predictable chaos of slow earthquakes. *Science advances*, **6 (27)**, eaaz5548.

Haarsma, R. J., and Coauthors, 2016: High resolution model intercomparison project (highresmip v1. 0) for cmip6. *Geoscientific Model Development*, **9 (11)**, 4185–4208.

Hersbach, H., and Coauthors, 2020: The era5 global reanalysis. *Quarterly Journal of the Royal Meteorological Society*, **146 (730)**, 1999–2049.

Hochman, A., P. Alpert, T. Harpaz, H. Saaroni, and G. Messori, 2019: A new dynamical systems perspective on atmospheric predictability: Eastern mediterranean weather regimes as a case study. *Science advances*, **5 (6)**, eaau0936.

Hochman, A., G. Messori, J. F. Quinting, J. G. Pinto, and C. M. Grams, 2021: Do atlantic-european weather regimes physically exist? *Geophysical Research Letters*, **48 (20)**, e2021GL095 574.

Ikehata, K., and M. Satoh, 2021: Climatology of tropical cyclone seed frequency and survival rate in tropical cyclones. *Geophysical Research Letters*, **48 (18)**, e2021GL093 626.

Kim, D., and Coauthors, 2018: Process-oriented diagnosis of tropical cyclones in high-resolution gcms. *Journal of Climate*, **31 (5)**, 1685–1702.

Klotzbach, P. J., M. M. Bell, S. G. Bowen, E. J. Gibney, K. R. Knapp, and C. J. Schreck III, 2020: Surface pressure a more skillful predictor of normalized hurricane damage than maximum sustained wind. *Bulletin of the American Meteorological Society*, **101 (6)**, E830–E846.

Knaff, J. A., and Coauthors, 2021: Estimating tropical cyclone surface winds: Current status, emerging technologies, historical evolution, and a look to the future. *Tropical Cyclone Research and Review*, **10**, 125–150, doi:https://doi.org/10.1016/j.tcrr.2021.09.002.

Knutson, T., and Coauthors, 2019: Tropical cyclones and climate change assessment: Part I: Detection and Attribution. *Bull. Amer. Meteor. Soc.*, **100**, 1987–2007, doi:10.1175/BAMS-D-18-0189.1.

Knutson, T., and Coauthors, 2020: Tropical cyclones and climate change assessment: Part ii: Projected response to anthropogenic warming. *Bulletin of the American Meteorological Society*, **101 (3)**, E303–E322.

Krishnamurti, T., S. Pattnaik, L. Stefanova, T. V. Kumar, B. P. Mackey, A. O'shay, and R. J. Pasch, 2005: The hurricane intensity issue. *Monthly weather review*, **133 (7)**, 1886–1912.

Landsea, C. W., and J. L. Franklin, 2013: Atlantic hurricane database uncertainty and presentation of a new database format. *Monthly Weather Review*, **141 (10)**, 3576–3592.

Lee, C.-Y., S. J. Camargo, A. H. Sobel, and M. K. Tippett, 2020: Statistical–dynamical downscaling projections of tropical cyclone activity in a warming climate: Two diverging genesis scenarios. *J. Climate*, **33**, 4815–4834, doi:10.1175/JCLI-D-19-0452.1.

Levich, E., and E. Tzvetkov, 1985: Helical inverse cascade in three-dimensional turbulence as a fundamental dominant mechanism in mesoscale atmospheric phenomena. *Physics reports*, **128 (1)**, 1–37.

Lorenz, E. N., 1990: Can chaos and intransitivity lead to interannual variability? *Tellus A*, **42 (3)**, 378–389.

Lucarini, V., D. Faranda, and J. Wouters, 2012: Universal behaviour of extreme value statistics for selected observables of dynamical systems. *Journal of statistical physics*, **147 (1)**, 63–73.

Lucarini, V., and Coauthors, 2016: *Extremes and recurrence in dynamical systems*. John Wiley & Sons.

Maraun, D., and M. Widmann, 2018: Cross-validation of bias-corrected climate simulations is misleading. *Hydrology and Earth System Sciences*, **22 (9)**, 4867–4873, doi:10.5194/hess-22-4867-2018, URL https://hess.copernicus.org/articles/22/4867/2018/.

Messori, G., and D. Faranda, 2021: Characterising and comparing different palaeoclimates with dynamical systems theory. *Climate of the Past*, **17 (1)**, 545–563.

Montgomery, M. T., and R. K. Smith, 2017: Recent developments in the fluid dynamics of tropical cyclones. *Annual Review of Fluid Mechanics*, **49**, 541–574.

Moon, Y., and Coauthors, 2020: Azimuthally averaged wind and thermodynamic structures of tropical cyclones in global climate models and their sensitivity to horizontal resolution. *J. Climate*, **33**, 1575 – 1595, doi:10.1175/JCLI-D-19-0172.1.

Muller, C. J., and D. M. Romps, 2018: Acceleration of tropical cyclogenesis by self-aggregation feedbacks. *Proceedings of the National Academy of Sciences*, **115 (12)**, 2930–2935.

Peng, M. S., B. Fu, T. Li, and D. E. Stevens, 2012: Developing versus nondeveloping disturbances for tropical cyclone formation. part i: North atlantic. *Monthly weather review*, **140 (4)**, 1047–1066.

Roberts, M. J., and Coauthors, 2020a: Impact of model resolution on tropical cyclone simulation using the HighResMIP–PRIMAVERA multimodel ensemble. *Journal of Climate*, **33 (7)**, 2557–2583.

Roberts, M. J., and Coauthors, 2020b: Projected future changes in tropical cyclones using the CMIP6 HighResMIP multimodel ensemble. *Geophysical Research Letters*, **47 (14)**, e2020GL088 662.

Robin, Y., M. Vrac, P. Naveau, and P. Yiou, 2019: Multivariate stochastic bias corrections with optimal transport. *Hydrology and Earth System Sciences*, **23 (2)**, 773–786.

Rotunno, R., Y. Chen, W. Wang, C. Davis, J. Dudhia, and G. J. Holland, 2009: Large-eddy simulation of an idealized tropical cyclone. *Bull. Amer. Meteor. Soc.*, **90**, 1783–1788, doi:10.1175/2009BAMS2884.1.

Schubert, S., and V. Lucarini, 2015: Covariant lyapunov vectors of a quasi-geostrophic baroclinic model: analysis of instabilities and feedbacks. *Quarterly Journal of the Royal Meteorological Society*, **141 (693)**, 3040–3055.

Simpson, R. H., and H. Saffir, 1974: The hurricane disaster potential scale. *Weatherwise*, **27 (8)**, 169.

Smith, A. B., and R. W. Katz, 2013: Us billion-dollar weather and climate disasters: data sources, trends, accuracy and biases. *Natural hazards*, **67 (2)**, 387–410.

Tang, J., D. Byrne, J. A. Zhang, Y. Wang, X.-t. Lei, D. Wu, P.-z. Fang, and B.-k. Zhao, 2015: Horizontal transition of turbulent cascade in the near-surface layer of tropical cyclones. *Journal of the Atmospheric Sciences*, **72 (12)**, 4915–4925.

Ullrich, P. A., C. M. Zarzycki, E. E. McClenny, M. C. Pinheiro, A. M. Stansfield, and K. A. Reed, 2021: Tempestextremes v2. 1: a community framework for feature detection, tracking and analysis in large datasets. *Geoscientific Model Development Discussions*, 1–37.

Vrac, M., 2018: Multivariate bias adjustment of high-dimensional climate simulations: the rank resampling for distributions and dependences (r 2 d 2) bias correction. *Hydrology and Earth System Sciences*, **22 (6)**, 3175–3196.

Vrac, M., P. Drobinski, A. Merlo, M. Herrmann, C. Lavaysse, L. Li, and S. Somot, 2012: Dynamical and statistical downscaling of the french mediterranean climate: uncertainty assessment. *Natural Hazards and Earth System Sciences*, **12 (9)**, 2769–2784.

Vrac, M., and S. Thao, 2020: R 2 d 2 v2. 0: accounting for temporal dependences in multivariate bias correction via analogue rank resampling. *Geoscientific Model Development*, **13 (11)**, 5367–5387.

Vulpiani, A., 2010: *Chaos: from simple models to complex systems*, Vol. 17. World Scientific.

Wolf, A., J. B. Swift, H. L. Swinney, and J. A. Vastano, 1985: Determining lyapunov exponents from a time series. *Physica D: Nonlinear Phenomena*, **16 (3)**, 285–317.

LIST OF TABLES

cc

Category	wind threshold [m/s]	minimum sea-level threshold [hPa]
1	33–42	>980
2	43–49	965–979
3	50–58	945–964
4	59–69	920–944
5	<69	<920

TABLE 1. Saffir-Simpson tropical cyclone intensity classification.

LIST OF FIGURES

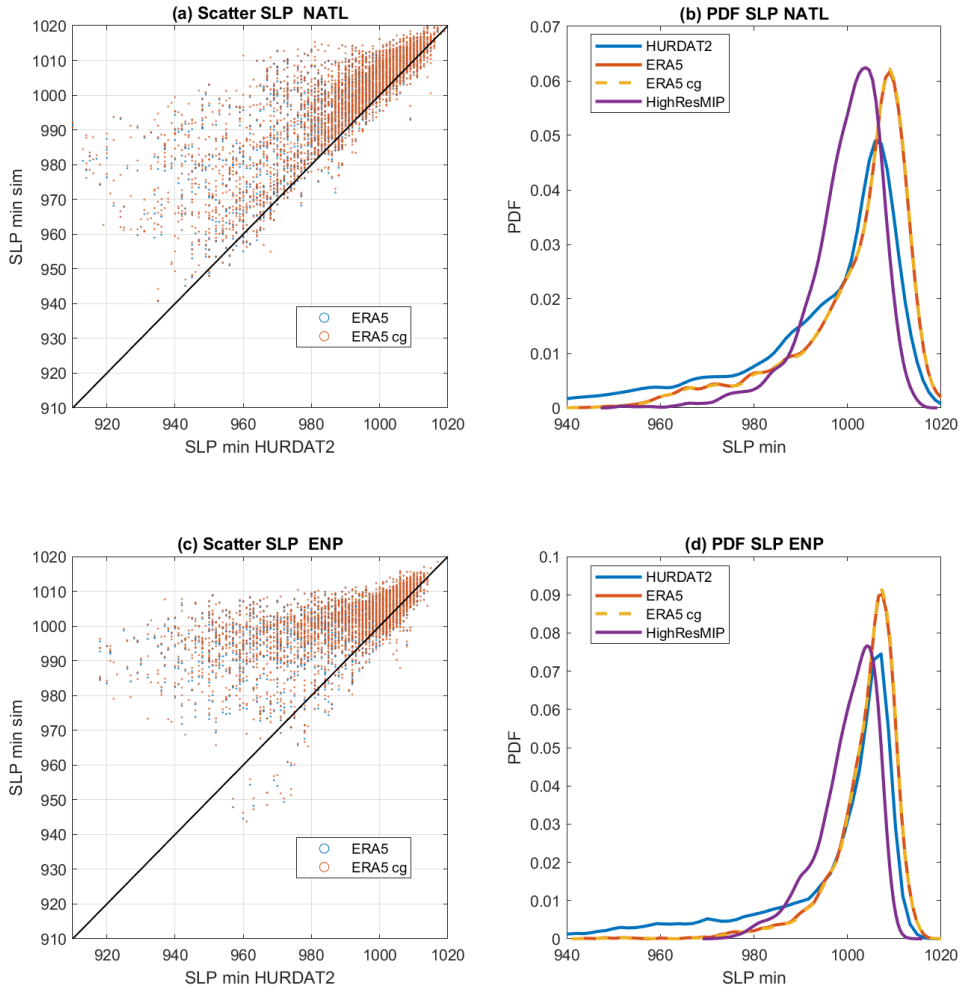

FIG. 1. Scatterplot of minimum SLP for (a) North Atlantic [NATL] and (c) Eastern North Pacific [ENP] tropical cyclones in HURDAT2 versus ERA5 and ERA5 cg. Probability density functions of minimum SLP for (b) North Atlantic and (d) Eastern North Pacific tropical cyclones in HURDAT2, ERA5, ERA5 cg and the IPSL-CM6A-ATM-ICO-HR model.

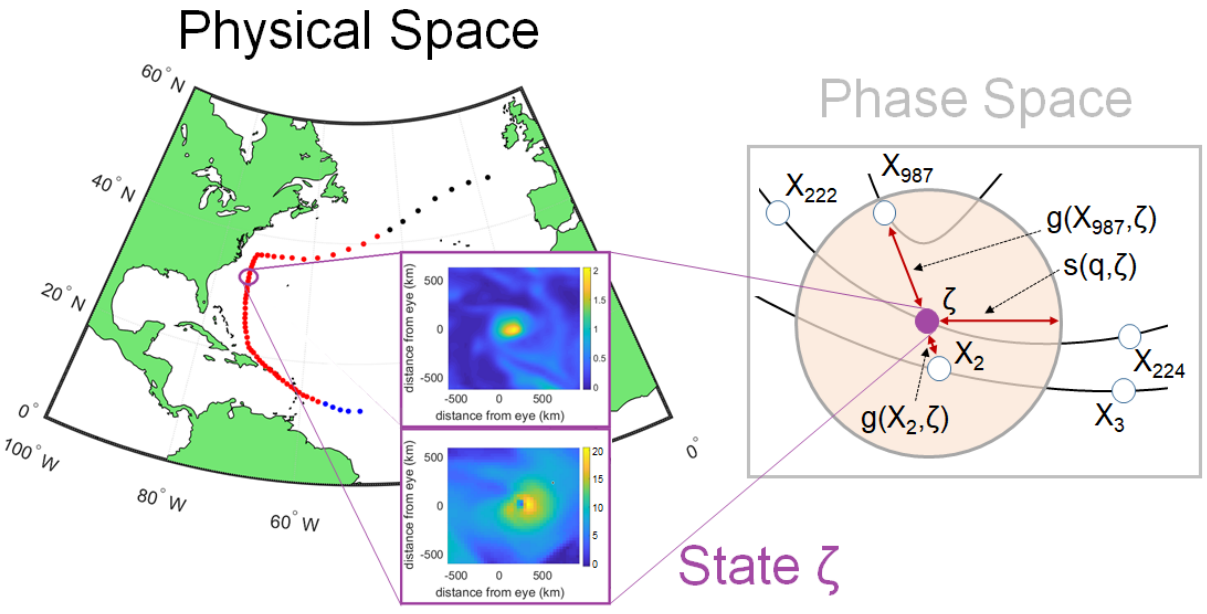

605 FIG. 2. Schematic of the computation of the dynamical systems metrics for an instantaneous state of a tropical
606 cyclone. We take a snapshot of the cyclone in physical space (black quadrant), in this example latitude–longitude
607 maps of *PV* and *uv* at 850 *hPa*, which correspond to state ζ in our phase space. The shaded circle is a 2D
608 representation of the hyper-sphere determined by the high threshold $s(q, \zeta)$, which defines recurrences of ζ.
609 The logarithmic distances between measurements defined by $g(X_i, \zeta)$ are marked by double-headed arrows. For
610 all points within the hyper-sphere, $g(X_i, \zeta) > s(q, \zeta)$ holds. In the schematic, only two measurements satisfy this
611 condition (adapted from (Messori and Faranda 2021)).

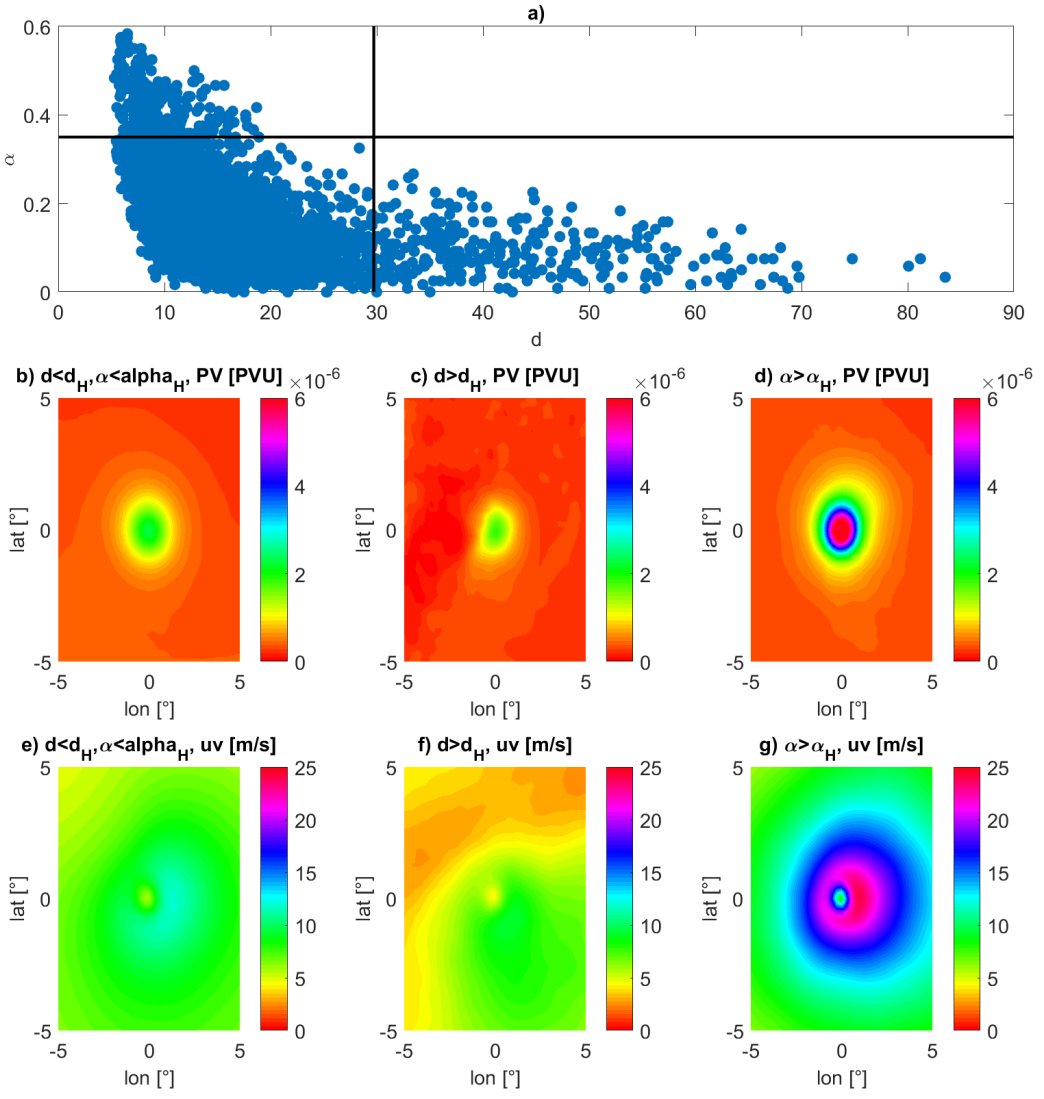

612 FIG. 3. The scatter plot displays the values of the instantaneous dimension d and the co-recurrence α com-
613 puted on ERA5 *uv* and *PV* maps during tropical cyclone timesteps in the NATL basin. The black solid lines mark
614 the 0.95 quantiles of the d and α distributions, namely d_H and α_H respectively. The maps show composites of
615 *PV* (b–d) and *uv* (e–g) for $d < d_H, \alpha < \alpha_H$ (b,e), $d > d_H$ (c,f) and $\alpha > \alpha_H$(d,g).

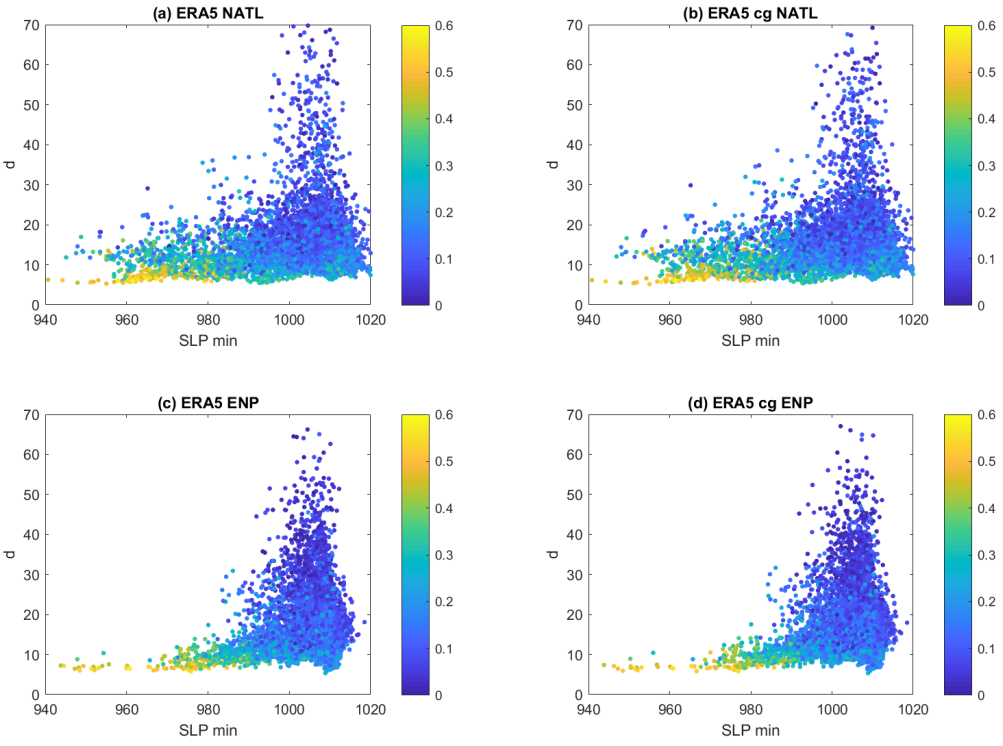

FIG. 4. Scatterplots of minimum SLP vs local dimension d and co-recurrence ratio α (colorscale) calculated on uv and PV at 850 hPa for (a,c) ERA5 and (b,d) ERA5 cg, in the (a,b) North Atlantic [NATL] and (c,d) Eastern North Pacific [ENP] basins.

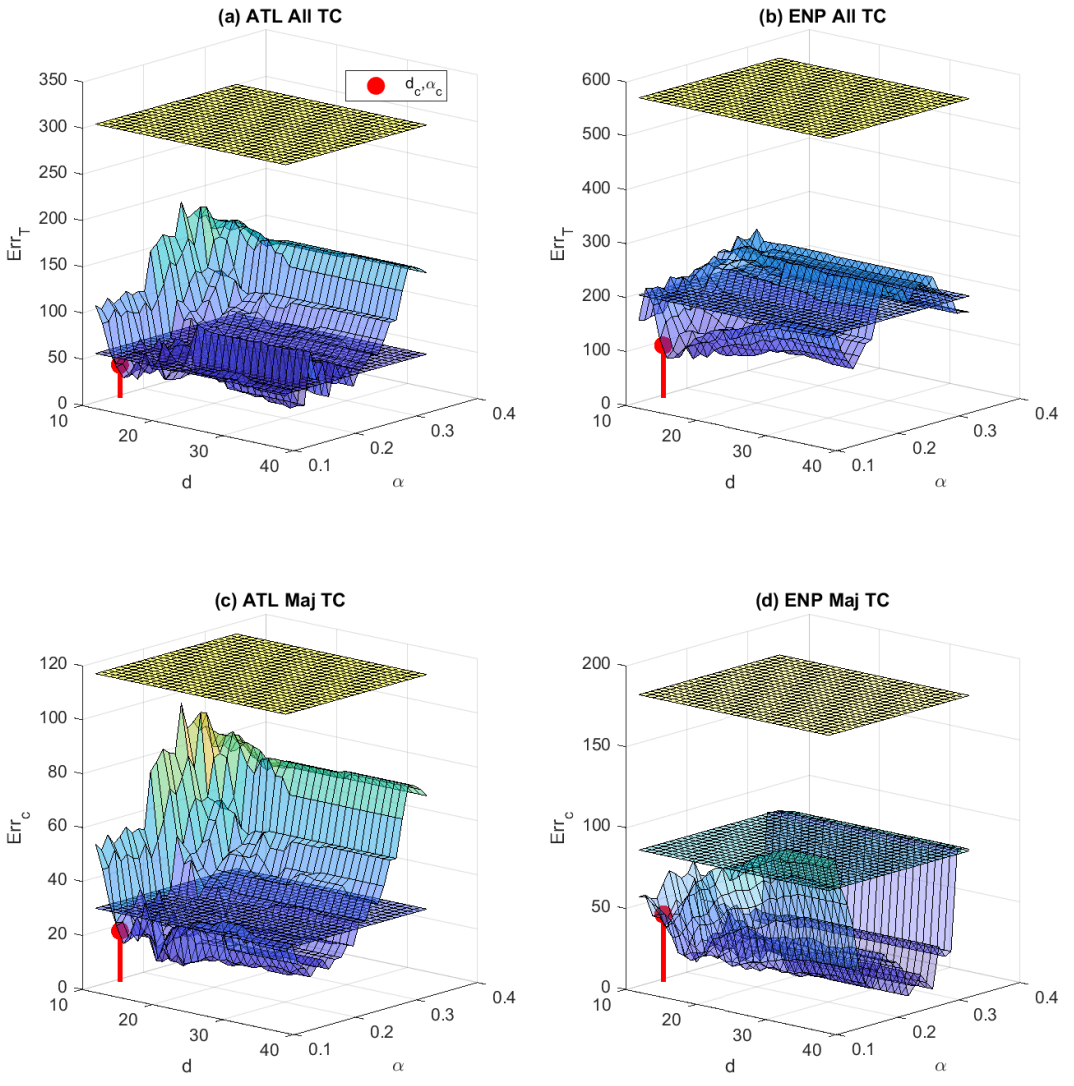

FIG. 5. Cyclone categorisation error for uncorrected ERA5 data, unconditional quantile–quantile correction and quantile–quantile correction conditioned on the dynamical systems metrics. The upper horizontal planes indicate the uncorrected errors, the lower horizontal planes the unconditional correction and the curved surface the dynamical systems corrections. (a,b) show errors for all intensity categories Err_T; (c,d) show errors for major tropical cyclones only Err_C. Panels refer to the (a,c) North Atlantic [NATL], and (b,d) Eastern North Pacific basin [ENP] basins. The red dots in the four panels show the chosen d_c–α_c values based on minimising the total error Err (see text). The vertical red lines show the points' projection on the d–α plane.

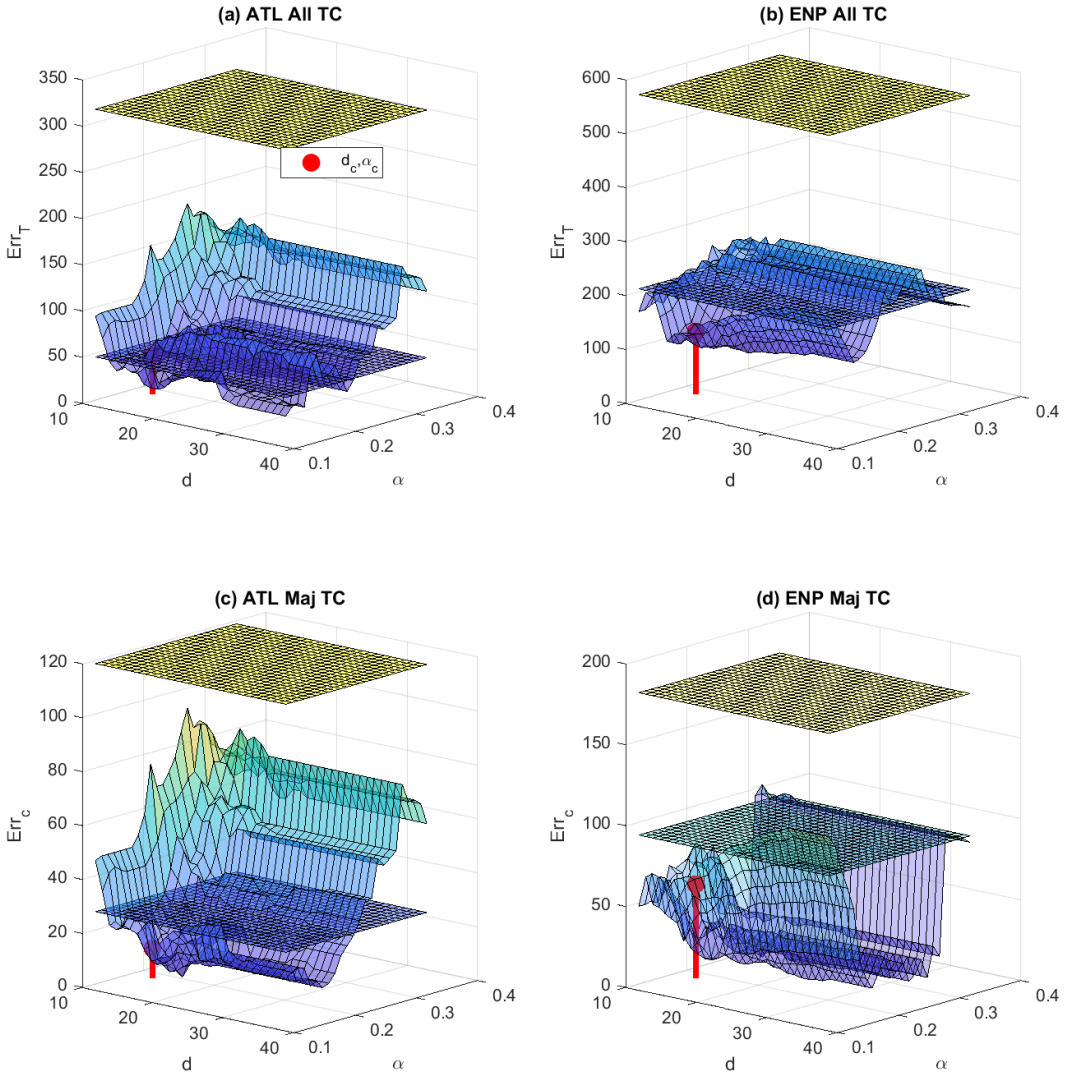

FIG. 6. As in Figure 5 but for the ERA5 cg data.

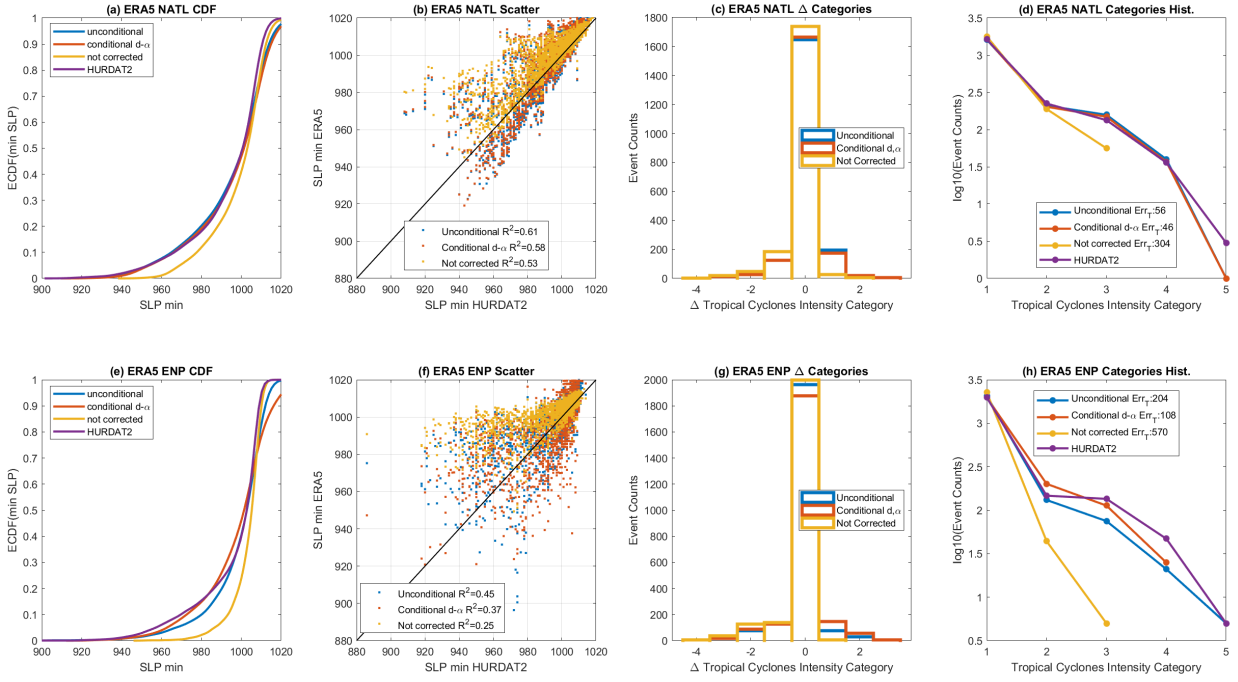

FIG. 7. Unconditional bias correction and bias correction conditioned on the dynamical systems metrics for the best d–α parameter combination (see Fig. 5, $\alpha_c = 0.11$, $d_c = 15$) for ERA5. (a,e) Empirical cumulative density functions (ECDFs), (b,f) scatter plots, (c,g) error in category intensities (negative values imply underestimation, positive values overestimation), (d,h) histogram of category intensities and ERR_T in the inset. (a-d) North Atlantic [NATL], (e-h) Eastern North Pacific [ENP] basins. See legends for details.

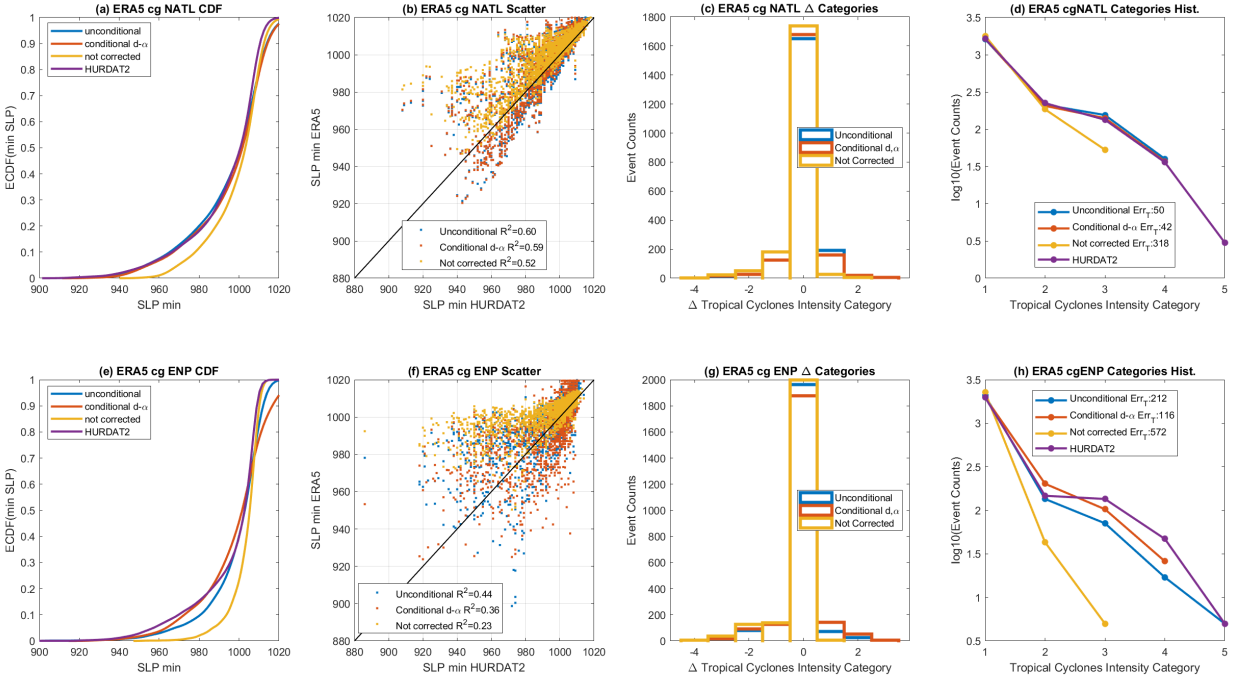

FIG. 8. As in Fig. 7 but for ERA5 cg data, using $\alpha_c = 0.13$, $d_c = 18$.

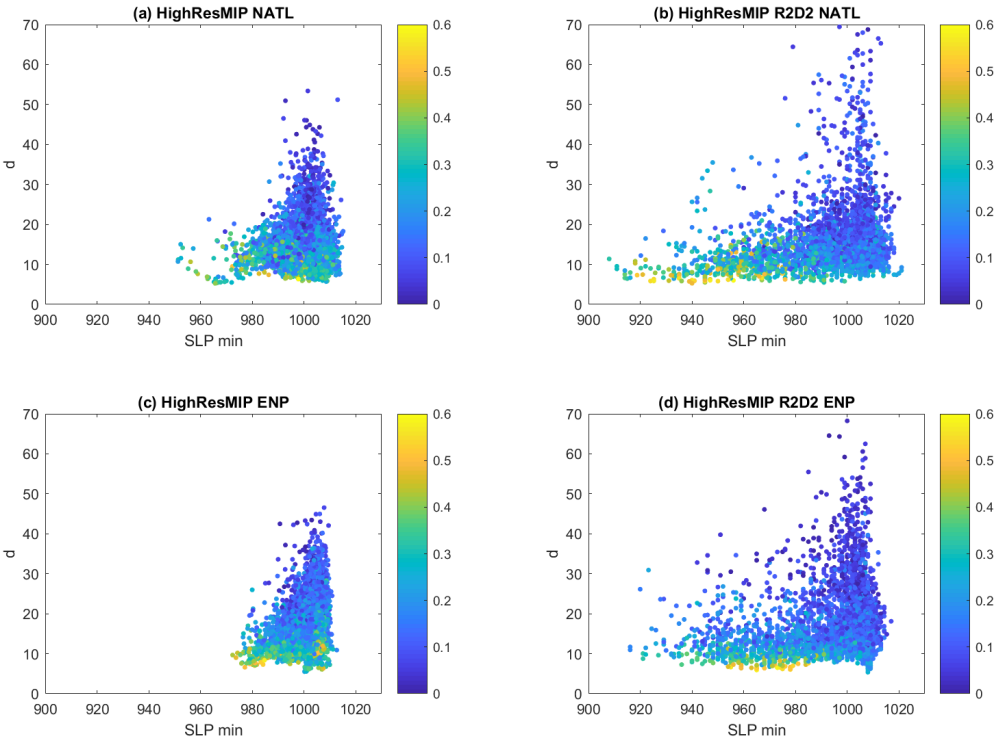

631 FIG. 9. Scatterplots of minimum SLP vs local dimension d and corecurrence ratio α (colorscale) calculated
632 on uv and PV at 850 hPa for (a,c) HighResMIP; (b,d) HighResMIP corrected with R2D2, in the (a,b) North
633 Atlantic [NATL] and (c,d) Eastern North Pacific [ENP] basins.

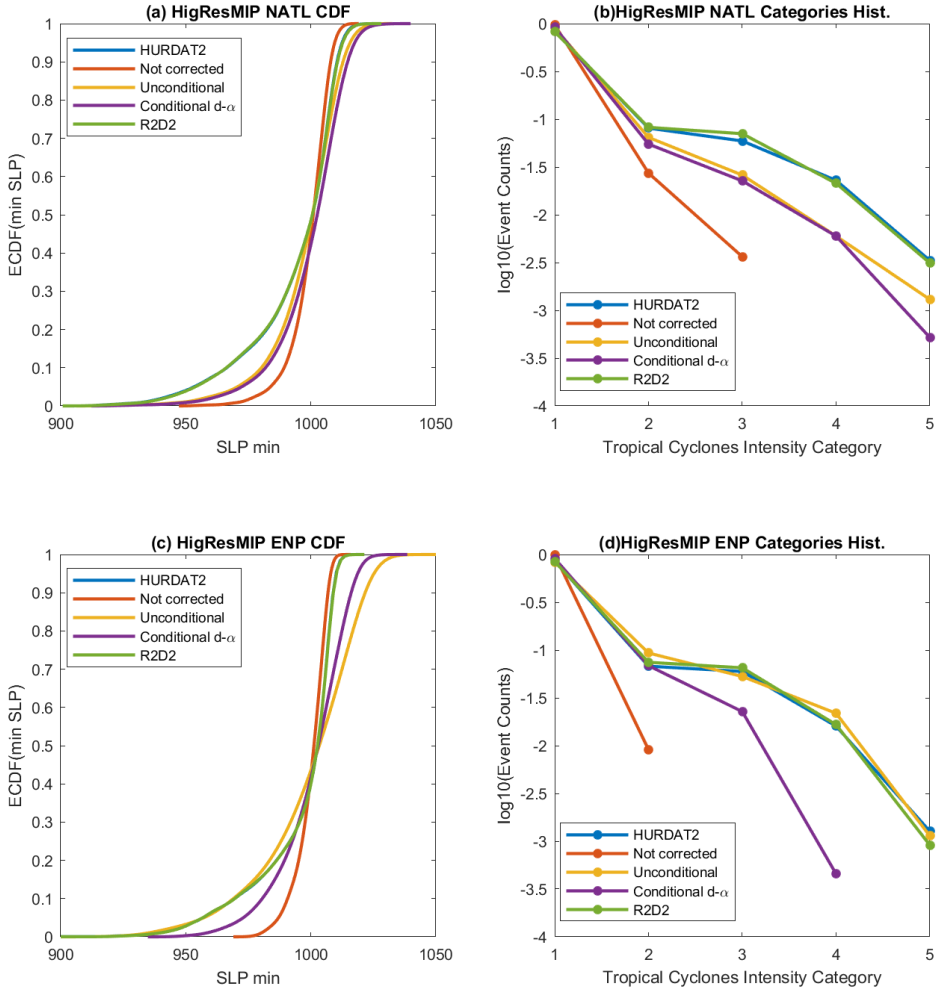

FIG. 10. Unconditional, R2D2, and conditional dynamical systems metrics bias corrections for the IPSL-CM6A-ATM-ICO-HR model. The conditional dynamical systems metrics bias corrections uses the best d–α parameter combination from ERA5 cg (see Fig. 6: $\alpha_c = 0.13$, $d_c = 18$.) Panels (a,c) show Empirical Cumulative Density Functions (ECDFs) and (b,d) histograms of category intensities for the North Atlantic [NATL] (a,b) and Eastern North Pacific [ENP] (c,d) basins.